Design and Distributed Computer Simulation of Thin p^+–i–n^+ Avalanche Photodiodes Using Monte Carlo Model

Mikhail Yakutovich

Belarussian State University

Abstract. The output current of an avalanche photodiodes (APD's) fluctuates in the absence of light as well as in its presence. The noise in APD's current arises from three sources: randomness in the number and in the positions at which dark carrier pairs are generated, randomness in the photon arrival number, and randomness in the carrier multiplication process. A Monte Carlo model has been used to estimate the excess noise factor in thin p^+–i–n^+ GaAs avalanche photodiodes. As this approach is computation intensive, simple parallel algorithm considering heterogeneous cluster based on MPICH was designed and implemented. Very good performance gain was achieved. It was found that APD model provides very good fits to the measured gain and noise and as such provides an accurate picture of the device operation. In this way, various device structures can be analyzed prior to their experimental realization. Through "computer experiments" like this outlined here, the effect of various geometries and material compositions on device performance can be assessed and optimal designs achieved.

1 Introduction

The avalanche photodiode (APD) is used in optical communications systems to convert a light signal into an electrical signal. The APD has internal gain, multiplying the signal current by the process of impact ionization in which a very energetic electron or hole creates a secondary electron-hole pair. A newly generated carrier must travel some distance (the dead space) in order to gain sufficient energy from the electric field to initiate an ionization event. The multiplication process introduces noise as a result of randomness in the ionization path length. The consequent variability in the generation of secondary carriers results in fluctuations in the total number of carriers produced per initial photocarrier, or multiplication. This noise component was first quantified by McIntyre [1,2] who found the following expression for the mean square noise current per unit bandwidth:

$$\langle i^2 \rangle = 2qI_p \langle M^2 \rangle F(\langle M \rangle) \tag{1}$$

where q is the electronic charge, I_p is the primary photo-current, $\langle M \rangle$ is the average current multiplication, and $F(\langle M \rangle)$ is the excess noise factor given by

$$F(\langle M \rangle) = k\langle M \rangle + (2 - 1/\langle M \rangle)(1 - k) \tag{2}$$

M. Bubak et al. (Eds.): ICCS 2004, LNCS 3039, pp. 515–522, 2004.

k is the ratio of the electron ionization coefficient α and the hole ionization coefficient β. If the primary photocarrier is a hole then $k = \alpha/\beta$ and if it is an electron then $k = \beta/\alpha$. However, recent experimental measurements on GaAs APD's [3,4,5,6] have shown a significant reduction in excess noise factor as i-region thickness decreases below one micron. A carrier starting with near zero energy, relative to the band edge, will have an almost zero chance of having an ionizing collision until it has gained sufficient energy from the electric field to attain the necessary energy to permit impact ionization [7,8]. Numerous analytical and numerical techniques have been proposed to address the nonlocal nature of impact ionization. Attempts to predict the ionization coefficients using Monte Carlo [9] and analytical techniques [10] have shown that, on average, carriers must travel a distance over which the potential drop is equivalent to $1.5 - 2$ times the ionization threshold energy before the probability of ionization, of a carrier which has not yet had an ionizing collision, rises to a steady-state, or "equilibrium," level.

Several techniques can potentially model the avalanche process while accounting for deadspace effects. These calculations would ideally be carried out using a Monte Carlo model with a full band structure (FBMC) calculated by the pseudopotential method, which provides the most realistic description of the transport. In recent years, full-band calculations have considerably advanced the understanding of impact ionization by showing that most carriers initiate events from higher lying bands producing secondary carriers with significant energy. The conventional Keldysh formula for the ionization rate, R_{ii} , which assumes a quadratic energy dependence, has also been shown to overestimate the ionization probability [11,12,13,14]. Stobbe [13] noted that different band structure assumptions can give different forms of the ionization rate which means that the accuracy of FBMC models for device simulations is questionable.

The lucky-drift (LD) model of Ridley [15,16] greatly simplifies the transport by using artificial trajectories based on the energy relaxation length which allows an analytic expression to be derived for the ionization coefficient. The complicated transport details are subsumed into a few material parameters which allows experimental results to be readily fitted and reveal a chemical trend. However, it was demonstrated in [17] that the use of energy relaxation path lengths to quantify phonon scattering in LD theory imposes a lower spatial limit of $0.1\mu m$. Furthermore, the model gives the incorrect spatial ionization probability which might lead to errors when calculating the excess noise factor associated with the avalanche process.

We used a simple Monte Carlo model (SMC) [18] for simulating thin APD's. It is an accurate, efficient and self-contained model for the avalanche process which can be used to predict both the multiplication and excess noise characteristics of all practical device geometries. Furthermore, this model allows experimental data to be fitted and interpreted with few parameters in a similar way to the LD model.

Since any Monte Carlo calculations are time consuming, which is especially restrictive when many ionization events need to be simulated to give reliable

statistics for the avalanche process, in this paper we present simple distribution algorithm. It takes into account the heterogeneous of cluster and allows achieving significant gain performance depending on contribution of any machine, independent of their relative speed.

Good results are shown between the calculated and measured multiplication and excess noise results from [3]. The simulation was tested on different heterogeneous clusters consisting of considerably different machines. Addition of relative "slower" machine leaded to achievement of gain, not deceleration. Our model can be used for simulation of complicated models utilizing relatively cheap clusters.

2 The Monte Carlo Model (MC)

We used a simple Monte Carlo model (SMC) [18] for simulating thin APD's. SMC uses single effective parabolic valleys and accurately accounts for deadspace effects. An effective parabolic valley is used for both electrons and holes which gives an energy independent mean-free path when phonon scattering is assumed to be solely by the deformation potential, which dominates at high electric fields.

To calculate the avalanche process in devices, the electric field profiles are generated in the depletion approximation assuming a built in voltage of $1.2V$. The values of the i-region thickness, w, the cladding doping, p^+ and n^+, and the unintentional p-type doping in the i-region, p^- were extracted from [6].

3 Estimation of Multiplication and Excess Noise Factor

The excess noise factor F is defined as the normalized second moment of the multiplication random variable M, when a single photocarrier initiates the multiplication. Thus,

$$F = \langle M^2 \rangle / \langle M \rangle^2 \tag{3}$$

where $\langle M \rangle$ is the mean multiplication and $\langle M^2 \rangle$ is the mean square multiplication.

The calculation uses an iterative scheme. The photo-generated electrons are first simulated yielding secondary electron and holes distributions. The secondary electrons are simply added to the electron simulation, and the calculation continues until all of the electrons are collected. The secondary hole distribution is then simulated based on the spatial of each particle's birth obtained from the initial electron simulation. Secondary holes arising from hole-initiated ionization effects are added to the hole simulation, and again, the calculation continues until all of the holes are collected. The electron simulation is then rerun with the secondary electrons. The total number of ionization events, N_t is recorded when all the carriers have left the multiplication region; the multiplication for that trial is then given by $M = N_t + 1$. By repeating the procedure for many trials, $\langle M \rangle$, and $\langle M^2 \rangle$ and F can be calculated. The number of trials is extended until successive values of differ by less than 0.0001. This usually requires at least 1000 trials for $\langle M \rangle = 2$ and $10000 - 50000$ trials for $\langle M \rangle$ larger than eight.

4 The Parallel MC Algorithm

Monte Carlo simulations of carrier transport in semiconductors are based on following the time evolution of an ensemble of particles through the material in both real and momentum space. The motion of each particle in the ensemble has to be simulated in turn, for the full duration of the simulation. It is assumed that these particles are effectively independent which makes the MC simulation well suited to parallel implementations to reduce computation time. The flow chart of a typical MC device simulation is shown in Fig. 1.

The parallel MC algorithm is based on a master-slave model [20]. The ensemble of particles is divided into subensembles, each of which is dedicated to a separate processor (slave). The slaves are solely responsible for simulating the particles' dynamics under the influence of the internal field distribution. The master processor updates the field distribution consistently with the port conditions enforced by the external circuitry. The master also serves as user interface. The MC algorithm will now be discussed with the aid of the flow chart (Fig. 2):

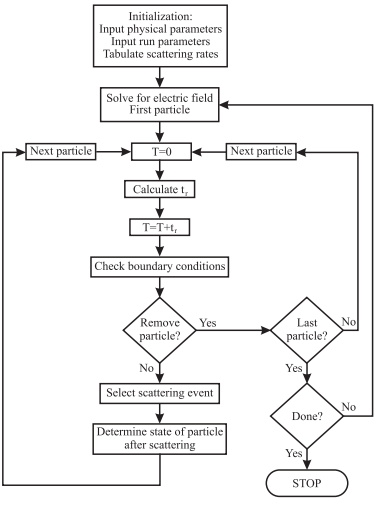

Fig. 1. Flow chart for a typical Monte Carlo device simulation algorithm

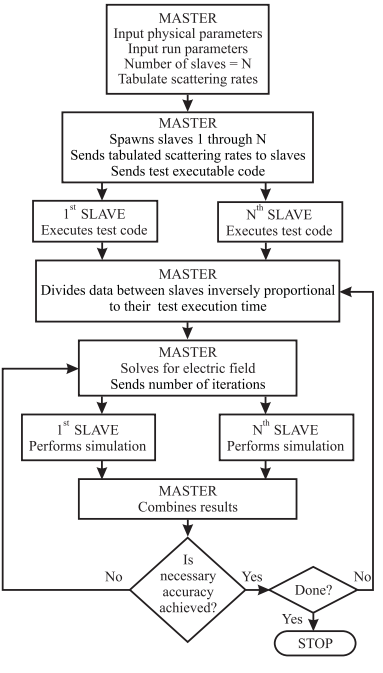

Fig. 2. Flow chart for a parallel MC device simulation algorithm

1. The master defines the physical device simulation problem and inputs the material and run parameters needed for the simulation. It also tabulates the various scattering rates as a function of particle energy.

2. The master spawns the slave executable code on N different slaves and sends the material parameters and tabulated scattering rates to each slave.
3. Each slave proceeds its own part until desired accuracy is attained.

To attain optimal efficiency, the computational load has to be shared among the processors in relation to their respective processing power. For a network of equally fast slave processors this implies that the number of particles in each subensemble must be kept equal throughout the simulation.

The main goal of dynamic load sharing is to equalize time τ_i of calculation on each slave machine, so the maximum theoretical performance gain will be achieved. Test computation performs on each machine before each simulation. Depending on test time τ_{ii}, the data is divided inversely proportional to τ_{ii}. So we can expand proposed algorithm:

1. The master defines the physical device simulation problem and inputs the material and run parameters needed for the simulation. It also tabulates the various scattering rates as a function of particle energy.
2. The master spawns the slave test executable code on N different slaves.
3. Each slave performs test code and sends execution time to master.
4. The master divides data between slaves inversely proportional to τ_{ii} and spawns the slave executable code on N different slaves and sends the material parameters and tabulated scattering rates to each slave.
5. Each slave proceeds its own part until desired accuracy is attained.

5 Results

The accuracy of the proposed parallel MC algorithm has been tested by comparing the results to those obtained by Plimmer [18]. The fit to the range of measured data for electrons and for holes is shown to be very good for M_e in Fig. 3 and for M_h in Fig. 4. In Fig. 5, the SMC-calculated excess noise factors are compared with the measured values from [3] for the range of p^+–i–n^+ structures with for the case of electron injection. This plot shows the calculated values to be in agreement with the measured results from [3] with the structure giving values close to those which would be predicted using the noise theory of McIntyre [1]. There is greater experimental uncertainties in measuring noise characteristics compared to the multiplication, but the MC predicts results close to experiment from all the diodes down to $0.1\mu m$ as shown on the plot.

The efficiency of the parallel SMC-algorithm have been quantified as the gain in computational speed achieved by employing multiple slaves relative to a master with single slave configuration and with different configurations. The modelling was executed on different homogeneous and heterogeneous clusters. The curves of the obtained speed-up as a function of the number of slaves are given in Fig. 6. In case of homogeneous cluster speed-up is close to ideal as our problem is perfectly suitable for parallelization.

Results of modelling in heterogeneous cluster are shown in Fig. 6 and Fig. 7. Every newly subsequent added computer had relatively lesser computing power.

The overall computing power of heterogeneous cluster was smaller then that of homogeneous cluster, hence, in general the overall speed-up in heterogeneous cluster reduced (Fig. 6). As it is shown in Fig. 7, our developed algorithm allowed efficiently distribute data between computers in a cluster, so the average idling time was greatly decreased. Addition of relative "slower" machine leaded to achievement of gain in any case. It is evident from the speed-up curves in Fig. 6 and Fig. 7 that the network communication plays a minor role in the efficiency of the algorithm, implying that a considerable improvement in computational speed is possible with the use of more powerful slave processors.

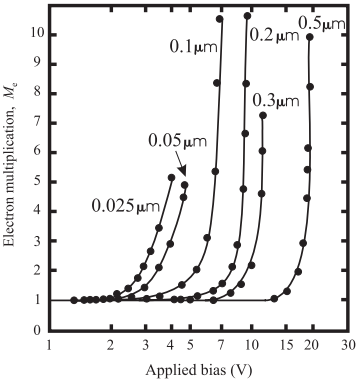

Fig. 3. Electron multiplication from MC calculations (•) compared against measured values (—) from pin's whose nominal i-region thicknesses are labelled on the plot

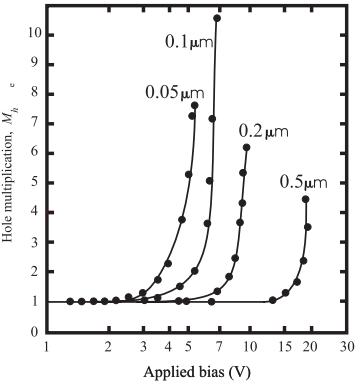

Fig. 4. Hole multiplication from MC calculations (•) compared against measured values (—) from pin's whose nominal i-region thicknesses are labelled on the plot

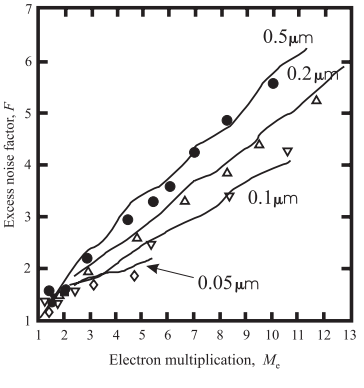

Fig. 5. SMC calculated excess noise, F, for electron injection from pin's with nominally $w = 0.5\mu m(\bullet)$, $0.2\mu m(\triangle)$, $0.1\mu m(\nabla)$ and $0.05\mu m(\diamondsuit)$ along with the measured results (—)

6 Conclusion

An efficient parallel implementation of the Monte Carlo particle simulation technique on a network of personal computers has been introduced. The parallel implementation have been successfully applied to the MC simulation of multiplication noise in GaAs p^+–i–n^+ avalanche photodiodes. These predict a decrease in excess noise factor as the multiplication length decreases from 1.0 to $0.05\mu m$ for both electron and hole injected multiplication. It was demonstrated that the excess noise factor depends strongly on the ionization path length distribution function.

Distributed computer simulation with dynamic load balancing greatly reduces computational time. Modelling was executed on different homogeneous and heterogeneous clusters. Addition of relative "slower" machine in heterogeneous cluster leaded to achievement of gain, not deceleration. Such algorithm can be widely used in different clusters.

Through "computer experiments" like this outlined here, the effect of various geometries and material compositions on device performance can be assessed and optimal designs achieved.

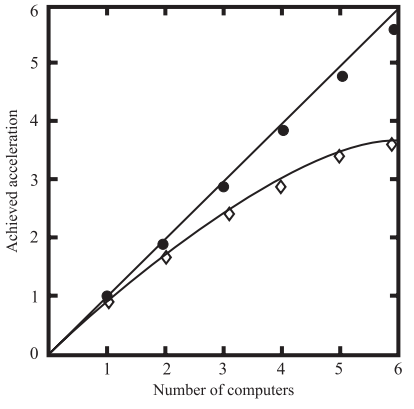

Fig. 6. The obtained speed-up curves for the MC-parallel algorithm in homogeneous (•) and heterogeneous (◇) clusters along with the ideal (—) speed-up curve

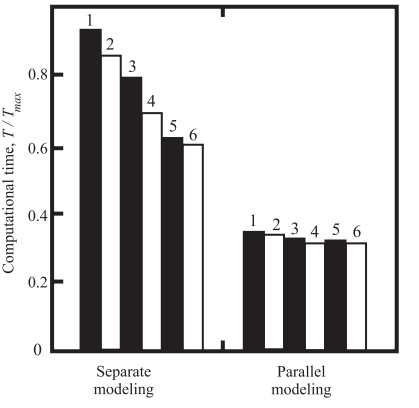

Fig. 7. Computational time for each processor working separately and in heterogeneous cluster

References

1. R. J. McIntyre, "Multiplication noise in uniform avalanche diodes," *IEEE Trans. Electron Devices*, vol. ED-13, Jan. 1966.
2. R. J. McIntyre, "The distribution of gains in uniformly multiplying photodiodes: Theory," *IEEE Trans. Electron Devices*, vol. ED-19, pp.703-713, 1972.

3. K. F. Li, D. S. Ong, J. P. R. David, G. J. Rees, R. C. Tozer, P. N. Robson, and R. Grey, "Avalanche multiplication noise characteristics in thin GaAs p^+–i–n^+ diodes," *IEEE Trans. Electron Devices*, vol. 45, pp. 2102-2107, Oct. 1998.
4. C. Hu, K. A. Anselm, B. G. Streetman, and J. C. Campbell, "Noise characteristics of thin multiplication region GaAs avalanche photodiodes," *Appl. Phys. Lett.*, vol. 69, pp. 3734-3736, 1996.
5. K. F. Li, D. S. Ong, J. P. R. David, P. N. Robson, R. C. Tozer, G. J. Rees, and R. Grey, "Low excess noise characteristics in thin avalanche region GaAs diodes," *Electron. Lett.*, vol. 34, pp. 125-126, 1998.
6. S. A. Plimmer, J. P. R. David, D. C. Herbert, T.-W. Lee, G. J. Rees, P. A. Houston, R. Grey, P. N. Robson, A. W. Higgs, and D. R. Wight, "Investigation of impact ionization in thin GaAs diodes," *IEEE Trans. Electron Devices*, vol. 43, pp. 1066-1072, July 1996.
7. Y. Okuto and C. R. Crowell, "Energy-conservation considerations in the characterization of impact ionization in semiconductors," *Phys. Rev. B*, vol. 6, pp. 3076-3081, 1972.
8. Y. Okuto and C. R. Crowell, "Ionization coefficients in semiconductors: A nonlocal property," *Phys. Rev. B*, vol. 10, pp. 4284-4296, 1974.
9. K. F. Brennan, "Calculated electron and hole spatial ionization profiles in bulk GaAs and superlattice avalanche photodiodes," *IEEE J. Quantum Electron.*, vol. 24, pp. 2001-2006, 1988.
10. A. Spinelli, A. Pacelli, and A. L. Lacaita, "Dead space approximation for impact ionization in silicon," *Appl. Phys. Lett.*, vol. 69, no. 24, pp. 3707-3709, 1996.
11. J. Bude and K. Hess, "Thresholds of impact ionization in semiconductors," *J. Appl. Phys.*, vol. 72, pp. 3554-3561, 1992.
12. N. Sano, T. Aoki, and A. Yoshii, "Soft and hard thresholds in Si and GaAs," *Appl. Phys. Lett.*, vol. 55, pp. 1418-1420, 1989.
13. M. Stobbe, R. Redmer, and W. Schattke, "Impact ionization rate in GaAs," *Phys. Rev. B*, vol. 49, pp. 4494-4497, 1994.
14. H. K. Jung, K. Taniguchi, and C. Hamaguchi, "Impact ionization model for full band Monte Carlo simulation in GaAs," *J. Appl. Phys.*, vol. 59, pp. 2473-2480, 1996.
15. B. K. Ridley, "Lucky-drift mechanism for impact ionization in semiconductors," *J. Phys. C: Solid State Phys.*, vol. 16, pp. 3373-3388, 1983.
16. B. K. Ridley, "A model for impact ionization in wide-gap semiconductors," *J. Phys. C: Solid State Phys.*, vol. 16, pp. 4733-4751, 1983.
17. S. A. Plimmer, J. P. R. David, and G. M. Dunn, "Spatial limitations to the application of the Lucky-drift theory of impact ionization," *IEEE Trans. Electron Devices*, vol. 44, pp. 659-663, Apr. 1997.
18. S. A. Plimmer, J. P. R. David, D. S. Ong, K. F. Li, "A Simple Model for Avalanche Multiplication Including Deadspace Effects," *IEEE Trans. Electron Devices*, vol. 46, April 1999.
19. L. V. Keldysh, "Kinetic theory of impact ionization in semiconductors," *Sov. Phys.-JETP*, vol. 10, pp. 509-518, 1960.
20. Robert R. van Zyl, Willem J. Perold, Hans Grobler "A Parallel Implementation of the Monte Carlo Particle Simulation Technique on a Network of Personal Computers"